Dynamic Adsorption and Tension of Nonionic Binary Surfactant Mixtures

Faisal A. Siddiqui and Elias I. Franses
School of Chemical Engineering, Purdue University, West Lafayette, IN 47907

For the first time, a model for dynamic adsorption and tension of diffusion-controlled systems has been extended to binary premicellar mixtures of nonionic surfactants of different adsorption capacities and nonideal interactions in the monolayer. Local equilibria between subsurface concentrations and adsorbate densities are modeled using the nonideal adsorbed solution theory, which describes these two elements. The model shows that larger molecules (those with the smaller adsorption capacity) tend to be preferentially adsorbed at low times, if they have equal adsorption equilibrium constants and diffusivities, and smaller molecules at longer times. This adsorption selectivity is reduced when larger molecules have a much larger adsorption equilibrium constant, or when there are negative deviations from ideality in the monolayer. This model's predictions are compared to tension data for two nonionic surfactants, $C_{12}E_5$ and Triton X-100, at 25°C. The data are represented well by the diffusion-controlled model with a finite diffusion-layer thickness, which describes the faster decrease in tension observed with the bubble surfactometer, compared to data with other techniques. With this model, surface coverages and concentration profiles are calculated, thus elucidating the adsorption selectivity of molecules of different adsorption capacities. Synergistic effects in dynamic tension and adsorption can be predicted. Mild synergism in dynamic tension lowering by the preceding nonionic surfactants is also observed.

Introduction

Dynamic adsorption and tension of surfactants at the air/water interface is important in foaming and foam stability (Bikerman, 1973; Garrett and Gratton, 1995), fast coating processes (Valentini et al., 1991), detergency (Schwuger, 1982), and lung surfactant function (Notter and Finkelstein, 1984). For such processes, the dynamics of adsorbed densities and surface tensions can be more important than the equilibrium behavior. Adsorption at other interfaces such as the liquid/liquid or the liquid/solid interface is important for emulsions, catalysis, and chromatography. Most surface-active formulations are mixtures of surfactants, lipids, polymers, or proteins, below or above the solubility or the critical micelle concentration (CMC). Surfactant mixtures can have quite different adsorption capacities and possibly nonideal mixing in the surface at high surface coverages, even though for dilute solutions the bulk solutions may be assumed to be ideally mixed. These factors must be considered in the dynamic adsorption problem.

Correspondence concerning this article should be addressed to E. I. Franses.

Equilibrium adsorption of one-component surfactants is well described by isotherms such as Langmuir, Frumkin (Borwankar and Wasan, 1983; Fainerman, 1991), or Freündlich (Scheindorf et al., 1981). Along with the Gibbs adsorption isotherm, they can describe equilibrium tension. If diffusion from the bulk to the subsurface layer (the liquid layer just below the surface) is much slower than the adsorption/desorption step from the subsurface to the surface layer, then the net absorption rate is said to be diffusion controlled, and "local equilibrium" is assumed between the subsurface and the interface, as reviewed recently (Miller et al., 1994; Chang and Franses, 1995). The diffusion-controlled problem for surfactant transport was first solved by Ward and Tordai (1946). Subsequently, other analytical or numerical solutions for various adsorption isotherms in modeling the local equilibrium were developed (Sutherland, 1952; Defay and Petré, 1971; Frisch and Mysels, 1983; Hua and Rosen, 1988; Kretzschmar and Miller, 1991; Fainerman and Miller, 1995). Whereas adsorption of nonionic surfactants is usually diffusion-limited, adsorption of ionic surfactants tends to be kinetic-limited

(Baret, 1968; Tsonopoulos et al., 1971; Miller and Kretzschmar, 1980; Borwankar and Wasan, 1983; Chang and Franses, 1991, 1995). In this article, we focus on solving the diffusion-controlled problem for binary mixtures of nonionic surfactants of different adsorption capacity and with nonideal mixing in the monolayer. The nonideal adsorbed solution (NAS) equilibrium model (Myers and Prausnitz, 1965; Siddiqui and Franses, 1996a) accounts generally for these factors.

To illustrate the important characteristics of surfactant size differences and nonideal mixing on dynamic adsorption, the new model was used for calculating equilibrium and dynamic tension and surface coverages for certain hypothetical mixtures (see the subsection titled "Sample Calculations"). The larger molecules are shown to selectively adsorb at small times, if they have equal adsorption equilibrium constants (equilibrium surface activities) and diffusivities. This selectivity is mitigated by negative deviations from ideal mixing, which decrease the desorption tendency of the larger molecules at longer times. Dynamic tension of two typical nonionic surfactants, $C_{12}E_5$ and Triton X-100, is shown to be diffusion-controlled, both for the individual components and for the mixtures. Tensions for these mixtures are compared to those calculated with the finite-thickness diffusion-controlled model. The model predicts well dynamic tension data for mixtures from pure-component equilibrium and dynamic parameters and one-equilibrium parameter for the mixture, with no new adjustable parameters. This model also predicts a phenomenon of "dynamic synergism," where the tension of the mixture is lower than that of either pure component at the same time and total concentration. Some mild dynamic synergism is observed with certain mixtures of the preceding surfactants.

Theory

Diffusion-controlled adsorption model for two surfactants

For binary mixtures of two nonionic surfactants below the CMC, the diffusion-controlled model is extended for the first time to molecules of different adsorption capacities and with nonideal mixing in the monolayer. Independent one-dimensional diffusion of components with diffusivities D_A and D_B is considered (Figure 1). It is assumed that there is a diffusion boundary layer in the solution and that the concentrations at $x = l$ are maintained constant at $c_i = c_i^e$ $(i = A, B)$; $x = 0$ is at the surface. This model can be applied to the case, $l \to \infty$, by using l much larger than the characteristic adsorption length, which is defined below. The finite-l model is useful for the bubble surfactometer method (see the third section), in which the diffusion distance is small and the interface is spherical. The surface densities $\Gamma_A(t)$ and $\Gamma_B(t)$ and the surface tension $\gamma(t)$ are assumed to be uniform.

The following two equations have been used for mixtures, in the literature primarily with the generalized Langmuir (g-L) isotherm (Ward and Tordai, 1946; Ziller and Miller, 1986; Dukhin et al., 1995; Chang and Franses, 1995), which uses the same adsorption capacities. Here they are used with the NAS model given below. In dimensionless form, the diffusion equations are

$$(N^l)^2 \frac{\partial u_A(\xi,\tau)}{\partial \tau} = \frac{\partial^2 u_A(\xi,\tau)}{\partial \xi^2} \tag{1}$$

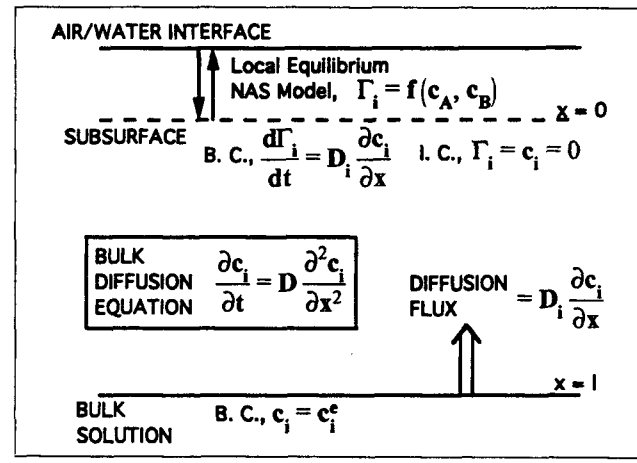

Figure 1. One-dimensional diffusion (no convection) equations and boundary conditions for two-components ($i = A, B$).

The subsurface concentration and the adsorbed surface densities are in local equilibrium, described by an implicit function from the NAS model, $\Gamma_i = f(c_A, c_B)$. The bulk solution is considered at uniform conditions (well-stirred). The thickness of the diffusion layer is l. The surface equation of state from the NAS model, $\gamma(\Gamma_A, \Gamma_B)$, allows for the calculation of surface tension.

$$(N^l)^2 R_D \frac{\partial u_B(\xi,\tau)}{\partial \tau} = \frac{\partial^2 u_B(\xi,\tau)}{\partial \xi^2}, \tag{2}$$

where u_i, τ, and ξ are the dimensionless concentrations, time, and distance from the surface:

$$u_i(\xi,\tau) \equiv \frac{c_i(x,t)}{c_i^e} \qquad i = A, B \tag{3}$$

$$\tau \equiv t \frac{D_A}{(\Gamma_A^e/c_A^e)^2} \tag{4}$$

$$\xi \equiv \frac{x}{l}, \tag{5}$$

R_D is the diffusivity ratio of the two components,

$$R_D \equiv \frac{D_A}{D_B}, \tag{6}$$

N^l is the dimensionless diffusion layer thickness,

$$N^l \equiv \frac{l}{(\Gamma_A^e/c_A^e)}, \tag{7}$$

where Γ_A^e and c_A^e are the surface density and the bulk concentration of A at equilibrium. The characteristic length for adsorption, Γ_A^e/c_A^e, represents the thickness of bulk solution containing sufficient material to cover the surface. At $x \gg \Gamma_A^e/c_A^e$, the bulk concentration is not perturbed from c_A^e. The limit $l \to \infty$ is achieved when l is larger than about $100(\Gamma_A^e/c_A^e)$. The ratio of the characteristic adsorption lengths is

$$R_X \equiv \frac{\Gamma_A^e/c_A^e}{\Gamma_B^e/c_B^e}. \tag{8}$$

Equations 10 and 11 are the boundary conditions at $\xi = 0$ in dimensionless form, with

$$\bar{\Gamma}_i \equiv \frac{\Gamma_i}{\Gamma_i^e} \qquad i = A, B \tag{9}$$

$$(N^l)\frac{d\bar{\Gamma}_A(\tau)}{d\tau} = \frac{\partial u_A(0,\tau)}{\partial \xi} \tag{10}$$

$$\left(N^l \frac{R_D}{R_X}\right)\frac{d\bar{\Gamma}_B(\tau)}{d\tau} = \frac{\partial u_B(0,\tau)}{\partial \xi}. \tag{11}$$

At $\xi = 1$ ($x = l$) the boundary conditions, $c_i = c_i^e$, result in

$$u_A(1,\tau) = 1 \tag{12}$$

$$u_B(1,\tau) = 1. \tag{13}$$

The initial conditions are:

$$\bar{\Gamma}_A(0) = \bar{\Gamma}_B(0) = 0 \tag{14}$$

$$u_A(0,0) = u_B(0,0) = 0 \tag{15}$$

$$u_A(\xi_{(\xi \neq 0)},0) = u_B(\xi_{(\xi \neq 0)},0) = 1. \tag{16}$$

Two additional conditions relating $\Gamma_i(t)$ to $c_i(0,t)$ are needed for completing the model (see the following subsection). They arise from the mechanism of adsorption, namely whether the adsorption rate is (1) diffusion-limited, (2) adsorption-desorption limited (or "slow adsorption"), or (3) a combination of (1) and (2) (or "mixed kinetics") (Van den Bogaert and Joos, 1980; Lin et al., 1990; Chang et al., 1992; Chang and Franses, 1992, 1995). The first case is developed here, since it represents the fastest possible net adsorption rate from a diffusion layer (with no convection effects). In this model, the rate is determined by D_A, D_B, l, and the preceding two conditions. The model uses the adsorption/tension equilibrium results that have been recently reported (Siddiqui and Franses, 1996a; Franses et al., 1995), and is expected to yield more reliable results than with the g-L isotherm. A summary of the equilibrium model is given below.

Nonideal adsorbed solution model

The Langmuir isotherm is used here in the data, the model being the simplest realistic isotherm for one component

$$\Gamma_i = \Gamma_{m,i}\frac{K_{L,i}c_i}{1 + K_{L,i}c_i}, \tag{17}$$

where $\Gamma_{m,i}$ are the adsorption capacities (the inverse of which are measures of molecular size and closest packing at the interface); $K_{L,i}$ are the adsorption equilibrium constants; and c_i are the concentrations in the bulk solution at equilibrium. In dimensionless form the Langmuir isotherm becomes:

$$\bar{\Gamma}_i = \frac{(1 + \bar{K}_{L,i})u_i}{1 + \bar{K}_{L,i}u_i} \qquad i = A, B \tag{18}$$

where

$$\bar{K}_{L,i} \equiv K_{L,i}c_i^e \tag{19}$$

The NAS model predicts mixture tension and adsorption behavior from the pure-components adsorption isotherms and certain additional mixing parameters (Siddiqui and Franses, 1996a). The model, developed by Myers and Prausnitz (1965) for gases on solids, relies on equating the chemical potentials of the surfactants in the bulk and at the interface and considering (for convenience) that mixing takes place at constant surface pressure. Nonideal interactions at the interface can be modeled with the regular solution equations or other mixing expressions, as indicated by the data. For pure components characterized by the one-component Langmuir isotherm, the following equations were derived (Siddiqui and Franses, 1996a), relating Γ_A and Γ_B to c_A and c_B in the form of two implicit equations. In dimensionless form,

$$\left(1 + \bar{K}_{L,A}\frac{u_A}{\zeta_A x_A}\right)^{R_\Gamma} = 1 + \bar{K}_{L,B}\frac{u_B}{\zeta_B x_B} \tag{20}$$

$$\frac{x_A(\zeta_A x_A + \bar{K}_{L,A}u_A)}{R_\Gamma \bar{K}_{L,A}u_A} + \frac{x_B(\zeta_B x_B + \bar{K}_{L,B}u_B)}{\bar{K}_{L,B}u_B} = \frac{\Gamma_{m,B}}{\Gamma_t}, \tag{21}$$

where x_i ($\equiv \Gamma_i/\Gamma_t$) is the mole fraction in the monolayer, Γ_t ($\equiv \Gamma_A + \Gamma_B$) is the total surface density, and ζ_i is the activity coefficient. For the regular solution model the activity coefficients are (Prausnitz et al., 1986)

$$\zeta_i = \exp\left[\beta^\sigma(1 - x_i)^2\right] \qquad i = A, B, \tag{22}$$

with β^σ being the interaction parameter. Negative β^σ indicates net attractive interactions in the mixed monolayer relative to the pure component monolayer. If $\Gamma_{m,i}$, $K_{L,i}$, and β^σ are specified, then x_A, x_B ($= 1 - x_A$), and Γ_t can be calculated from Eqs. 20–22. Then the surface densities $\Gamma_i = x_i\Gamma_t$ and the surface tension γ are calculated, the latter from the equation

$$\gamma = \gamma_0 - \Gamma_{m,a}\,\mathcal{R}T\ln\left(1 + \frac{\bar{K}_{L,A}u_A}{x_A\zeta_A}\right). \tag{23}$$

Equations 20, 21, and 23 were derived by Siddiqui and Franses (1996a). For molecules of the same adsorption capacity, $\Gamma_{m,A} = \Gamma_{m,B}$, and for ideal mixing at the interface ($\zeta_i = 1$ or $\beta^\sigma = 0$), Eqs. 20 and 21 reduce to the explicit relations known as the g-L isotherm. This isotherm (similar to Eq. 17, but with the term $\Sigma_i K_{L,i}c_i$ in the denominator) should not be used for $\Gamma_{m,A} \neq \Gamma_{m,B}$, since then it violates the Gibbs-adsorption isotherm, that is, it is thermodynamically inconsistent (Broughton, 1948; LeVan and Vermeulen, 1981; Franses et al., 1995).

The NAS model (or its ideal limit, the ideal adsorbed solution (IAS) model) can be used for calculating surface cover-

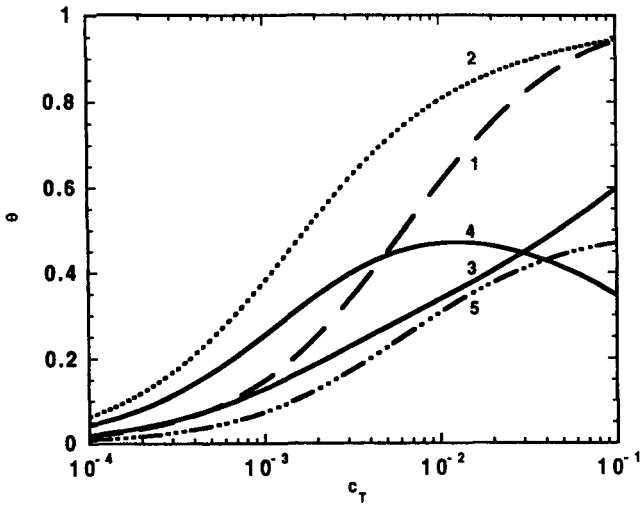

Figure 2. Surface coverage predictions ($\theta \equiv \Gamma_i/\Gamma_{m,i}$) of the generalized-Langmuir (g-L) isotherm and of the NAS model.

Curve 1 corresponds to pure A, or pure B, or the total coverage for the mixture ($\theta_T \equiv \theta_A + \theta_B$) for the g-L isotherm. Curve 2 is the surface coverage of θ_A or θ_B individually for the Langmuir isotherm; Curves 3 and 4 are surface coverages for A and B, respectively, for the NAS model, and curve 5 is $\theta_T \equiv \theta_A + \theta_B$ for the NAS model; $\Gamma_{m,A} = 9\times10^{-6}$ mol/m^2, $R_\Gamma = 3$, $R_K = 1$, $y_A = 0.5$. For the NAS model, $\beta^\sigma = -5$ was used.

ages for molecules of different $\Gamma_{m,i}$ and for $\beta^\sigma \neq 0$. The g-L isotherm cannot describe nonidealities or differences in adsorption capacities. Its predictions differ substantially from those of the IAS model (Franses et al., 1995). With the NAS model it is possible to make thermodynamically plausible predictions of surface coverages and compositions, and describe phenomena such as surface-tension-reduction synergism, in which the surface tension of the mixture is less than that of either pure component at the same total concentration (Siddiqui and Franses, 1996b). The adsorption capacity for mixtures has been reported by Siddiqui and Franses (1996a,b).

Equilibrium tension data for pure components can be fitted for obtaining $\Gamma_{m,i}$ and $K_{L,i}$. Data for mixtures can be used for determining the validity of the NAS model and the surface interaction parameter (β^σ) of the regular solution. With these parameters, one can predict equilibrium surface coverages for binary mixtures. In Figure 2, the surface area coverages $\theta_i \equiv \Gamma_i/\Gamma_{m,i}$ are shown for a hypothetical mixture for which $\Gamma_{m,A} = 9\times10^{-6}$ mol/m^2, $R_\Gamma = 3$, $R_K = 1$, and $y_A = 0.5$. The total coverage is higher for the mixture than for the individual pure components (curve 1) at the same total concentration, indicating synergistic adsorption. At the conditions shown, the larger molecule (B, curve 4) adsorbs preferentially at low concentrations, but less at higher concentrations. The surface coverages calculated using the NAS model are quite different from those calculated with the g-L isotherm.

Details of numerical solution for diffusion-controlled model

Equations 1, 2, and 10–16 were solved along with Eqs. 20–22, which were applied for $\Gamma_A(t)$ and $\Gamma_B(t)$ as a function of $c_A(0,t)$ and $c_B(0,t)$, for obtaining the surface densities and the concentration profiles. The dynamic surface tension was then calculated from Eq. 23, which was applied for $\gamma(t)$ as a function of $\Gamma_A(t)$ and $\Gamma_B(t)$. An implicit finite difference scheme with a variable spatial grid was used, since the concentration profiles near the interface ($\xi = 0$) at small τ-values change quite rapidly. A very fine grid is used near the surface, and a coarse grid is used away from the interface (Siddiqui, 1996).

The finite difference method was used iteratively starting with an initial guess for the subsurface concentration $[u_i(0,\tau)]$. The entire concentration profile was then calculated with the finite difference scheme. At each time step, the concentration gradient at the interface $(\partial u_i/\partial\xi|_{\xi=0})$ was calculated with the tri-diagonal matrix algorithm (Thomas, 1949). The iterative scheme was stopped when the concentration gradients at $\xi = 0$ and the time derivatives of the surface densities (Eqs. 10 and 11) differed by less than 10^{-8}. The program was tested for accuracy with Henry's law isotherm (the low concentration limit for both the g-L isotherm and the NAS model), for which an analytical solution is available (Sutherland, 1952). Since no general analytical results were derived, sample calculations were done for providing some useful insights on possible dynamic adsorption behavior and for comparing the models.

Sample calculations

In Figures 3–5, a hypothetical binary mixture with parameters similar to those of typical nonionic surfactants is considered, for illustrating diffusion-controlled adsorption model using the NAS model for the local equilibrium at the surface. Surfactant A (the "smaller" molecule or the molecule with the smaller packing density) has an adsorption capacity $\Gamma_{m,A} = 9\times10^{-6}$ mol/m^2 (≈ 18 Å^2/molecule), which is three times

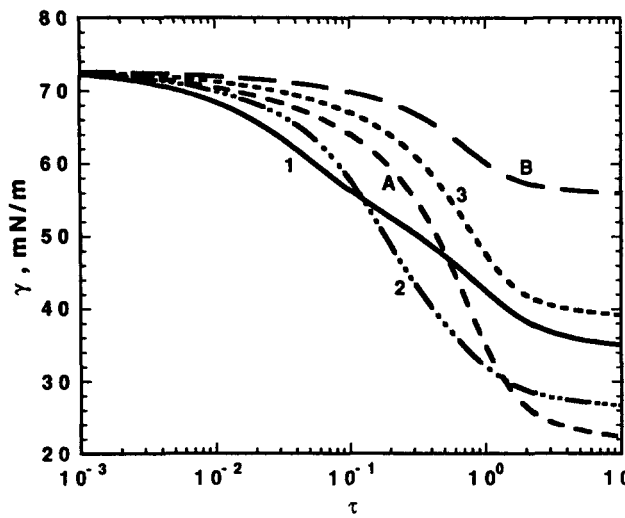

Figure 3. Tension predictions for the IAS (curve 1) and the NAS model (curve 2, with $\beta^\sigma = -5$) for $R_\Gamma = 3$, $R_K = 1$, $R_D = 1$, and $\Gamma_{m,A} = 9\times10^{-6}$ mol/m^2.

Curves A and B are for one component Langmuir isotherm, and curve 3 is for the g-L isotherm, which is thermodynamically inconsistent (LeVan and Vermeulen, 1981; Franses et al., 1995). The dimensionless time, $\tau \equiv D_A t/(\Gamma_A^s/c_A^s)^2$.

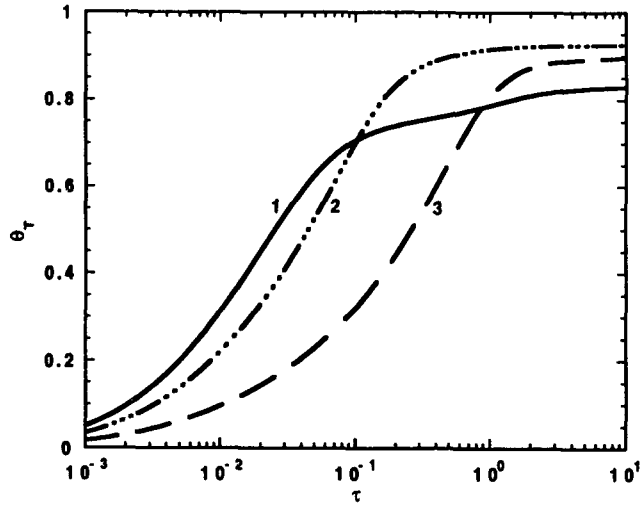

Figure 4. Area coverages, $\theta_T \equiv \theta_A + \theta_B$ for the three models in Figure 3.

Curves for pure A and pure B are the same as curve 3.

greater than that of surfactant B (the "larger" molecule), with $\Gamma_{m,B} = 3 \times 10^{-6}$ mol/m^2 (≈ 56 Å^2/molecule). All other parameters such as the equilibrium adsorption constant $K_{L,i}$, diffusion coefficient D_i, and bulk concentrations were taken equal for the two components for these sample calculations. Because of its larger adsorption capacity, surfactant A reduces the tension to a lower value (22 mN/m) than surfactant B (56 mN/m, Figure 3).

It can be argued that the "larger" molecules may be more hydrophobic and have larger adsorption equilibrium constants. This can indeed mitigate the effect of smaller adsorption capacity on equilibrium adsorption, as shown previously (Franses et al., 1995; Siddiqui and Franses, 1996a). Moreover, if the size also affects the diffusivity significantly, it can affect also the adsorption dynamics. If the surfactant components belong to the same homologous series, then one would expect as the chain length increases that Γ_m may decrease slightly and K_L may increase substantially. If the components' molecular structures are not closely related, however, then Γ_m and K_L are not necessarily related.

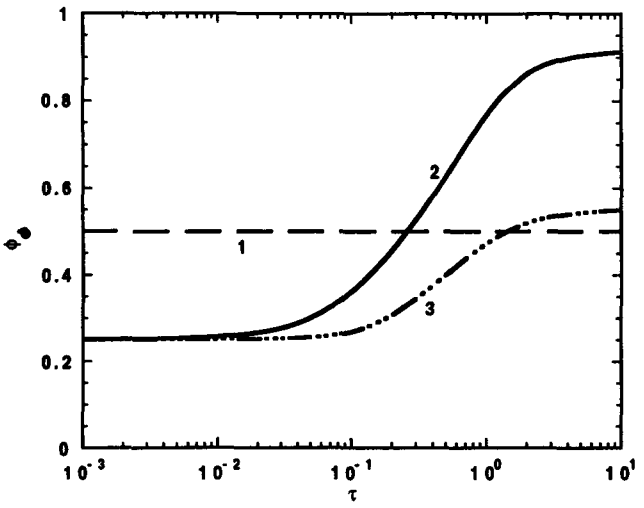

Figure 5. Fractional area coverages, $\phi_A \equiv \theta_A/(\theta_A + \theta_B)$, for the three models in Figure 3.

Curves for pure A and pure B are the same as curve 3.

In Figure 3 an equimolar mixture of A and B is considered for comparing the ideal adsorbed solution model with the nonideal adsorbed solution model and the g-L isotherm. The first model, which considers size differences but no net interactions at the interface ($\beta^\sigma = 0$), predicts a lower dynamic surface tension than either pure A or pure B at low timescales. This phenomenon is termed synergism in dynamic tension. Dynamic-tension synergism is also predicted at small times by the NAS model (here with $\beta^\sigma = -5$, even though no synergism in the equilibrium surface tension is predicted. For the g-L isotherm (in which the average $\bar{\Gamma}_m = 6 \times 10^{-6}$ mol/m^2 was used for calculating tensions), the predicted dynamic surface tensions are intermediate between those of pure A and pure B, and quite different from those of the IAS model.

Figure 4 shows the total area coverages, $\theta_T \equiv \theta_A + \theta_B$ ($\theta_i \equiv \Gamma_i/\Gamma_{m,i}$), for the systems in Figure 3. The area coverages for the g-L isotherm are the same as those for pure A or pure B. The coverages for the IAS model are higher (synergistic dynamic adsorption) than those of A or B alone for τ up to about 7. Those for the NAS model are higher (synergistic) at all timescales.

The fractional area coverages of component A, $\phi_A \equiv \theta_A/(\theta_A + \theta_B)$, are quite different for the IAS and the NAS models (Figure 5): $\phi_A < 0.5$ at small times and $\phi_A > 0.5$ at large times, as the larger molecules desorb yielding space to the smaller molecules, which are more surface active (and more efficient in lowering tension). For the ideal mixing model, the smaller molecules have greater coverage than for nonideal mixing: $\phi_A = 0.91$ vs. 0.55 at equilibrium. The net attractive interactions between the molecules ($\beta^\sigma = -5$) make the desorption of the larger molecules at higher concentrations, and the increased adsorption of the larger molecules, less likely than when only size differences matter. In contrast, the g-L isotherm-based model predicts no composition variation with time. Only the NAS model will be applied below to describe data of a binary nonionic surfactant mixture.

Materials and Methods

Two nonionic surfactants, isomerically pure (99%) $C_{12}E_5$ [$CH_3(CH_2)_{11}(OCH_2CH_2)_5$–OH] and Triton X-100 [$(CH_3)_3CCH_2C(CH_3)_2C_6H_4(OCH_2CH_2)_{9.5}OH$] were obtained from Fluka Chemicals and from Sigma chemicals, respectively, and were used as received. Although Triton X-100 is a polydisperse mixture, it is well characterized by the one-component Langmuir isotherm for equilibrium tension (Lin et al., 1990; Chang and Franses, 1994a) and for dynamic tension behavior. It can (and will) be considered effectively as a single-component surfactant. Pure water with an initial resistivity of 18 MΩ·cm from a Milli-Q (Millipore) four-stage cartridge system (ion exchange, organic adsorption, ultrafiltration), was used.

Dynamic surface tensions were measured with the pulsating bubble surfactometer (Electronetics, Buffalo, NY), which measures the pressure difference across a bubble interface (Enhorning, 1977). The Laplace–Young equation, $\Delta P =$

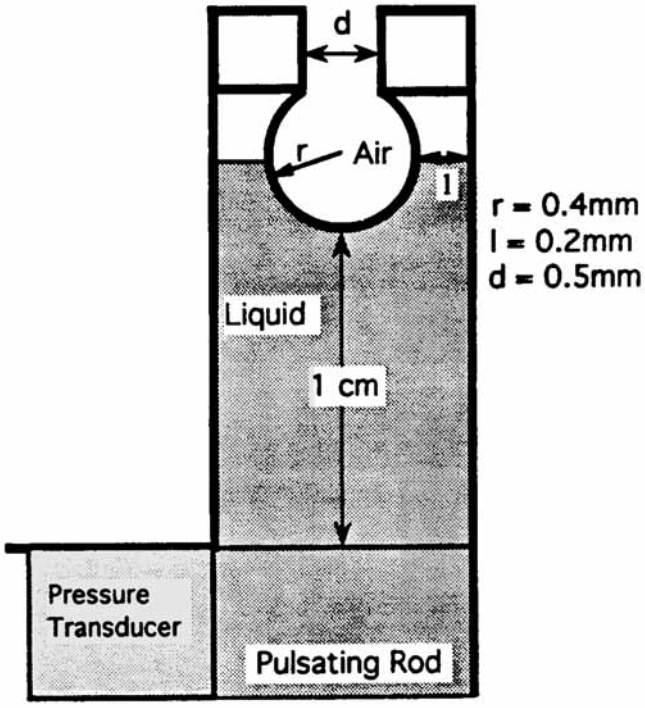

Figure 6. The bubble surfactometer (not to scale) (Electronetics, Buffalo, NY) used to measure surface tensions.

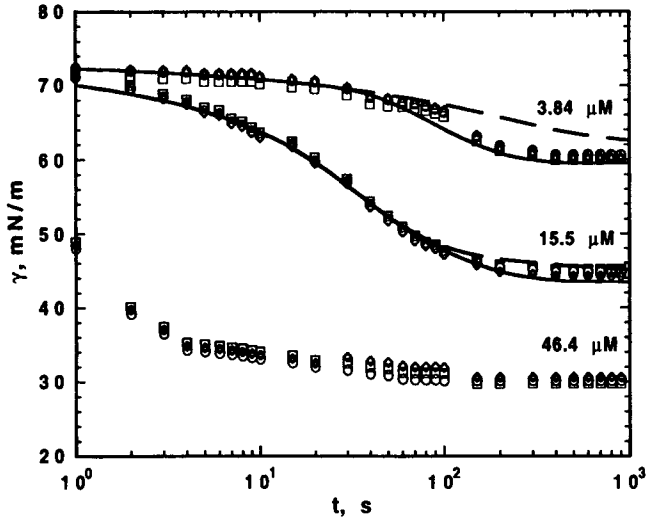

Figure 7. Dynamic surface tensions of aqueous $C_{12}E_5$ at 25°C with the PBS method.

The different symbols in each group of data (○, □, ◇) represent independent runs and the estimated error is ±1 mN/m. Solid lines represent data fits to a flat-interface, diffusion-controlled model with nearly infinite length ($N^l = 100$); broken lines represent a model of finite thickness, $l = 0.02$ cm, for $c_T = 3.84$ ($N^l = 0.21$) and 15.5 μM ($N^l = 0.5$), respectively. The data for 46.4 μM were not fitted because the concentration is above the cmc (40 μM). $D = 3.0 \times 10^{-10}$ m²/s (see text).

$2\gamma/R$, was used for calculating the surface tension when γ varies with time. The method has been described and analyzed before in detail (Chang and Franses, 1994a,b). The bubble radius is 0.4 mm. The distance from the side of the bubble to the sample chamber wall is ca. 0.2 mm, and the distance to the bottom of the chamber is 1 cm (Figure 6). Data acquisition starts 1 s after a bubble is formed at a sampling interval of 0.05 s. Data were obtained at 25 ± 1°C. Equilibrium data were also obtained using the Krüss tensiometer with a Wilhelmy plate and have been reported previously (Siddiqui and Franses, 1996a).

Dynamic tension data, obtained using the bubble surfactometer method for a spherical interface, are compared to calculations made with the model for a planar interface. If the radius of the bubble is much greater than the characteristic adsorption length Γ_A^e/c_A^e, then using a finite-length planar interface model instead of a spherical interface makes little difference (Chang and Franses, 1994b). The sphericity of the interface could increase the adsorption rate over the planar interface only when Γ_A^e/c_A^e is comparable or smaller than the radius of the bubble (Chang and Franses, 1994a). In the following section the data obtained with the bubble method are compared to calculations made by the adsorption model with either finite or infinite diffusion length.

Experimental Results and Comparison to the Models

Dynamic tension data for pure $C_{12}E_5$ (Figure 7) are shown for three different concentrations, from 3.84 to 46.4 μM. Whereas the first two solutions equilibrate in approximately 200 s, the 46.4-μM solution equilibrates within ca. 10 s. Since the 46.4-μM concentration is above the CMC (Carless et al., 1964), these data were not fitted with the present model, which applies only to molecular solutions. The $C_{12}E_5$ data were fitted with the infinite-l (broken line) and the finite-l (solid line) models for the diffusion-controlled mechanism, with Γ_m and K_L determined previously: for $C_{12}E_5$, $\Gamma_{m,A} = 8.0 \times 10^{-6}$ mol/m², $K_{L,A} = 2.2 \times 10^2$ m³/mol, and for Triton X-100, $\Gamma_{m,B} = 2.8 \times 10^{-6}$ mol/m², and $K_{L,B} = 1.8 \times 10^3$ m³/mol (Siddiqui and Franses, 1996a). In this case, Triton X-100, which is the "larger" molecule (smaller Γ_m), has a larger value of K_L. The diffusion coefficient was estimated, from the accepted value of $D = 2.6 \times 10^{-10}$ m²/s for Triton X-100 and the molecular weights, to be 3.0×10^{-10} m²/s by using the Stokes-Einstein equation, in which D is inversely proportional to the cube root of the molecular weight (Bird et al., 1960). Dynamic tensions as calculated with the infinite-l model drop more slowly than the data. A finite-l model, with $l = 0.2$ mm (the distance from the surface to the wall of the container, Figure 6), was used for calculating dynamic tensions that fit the data better.

The equilibrium times for Triton X-100 at the same concentrations as for $C_{12}E_5$ are 400, 100, and 20 s for 3.84, 15.5, and 46.4 μM, respectively (Figure 8). The data reproduce well those obtained previously in our laboratory for the same concentrations and with the same apparatus (Chang and Franses, 1994a). Data obtained by Lin et al. (1990), who used the digitized emerging-bubble (or inverted pendant-drop) method, show longer equilibrium timescales than our data (Figure 8). Predictions from the infinite-l model fit the data of Lin et al. fairly well, and the finite-l model represents our data better by using the same diffusion coefficients. One infers that the intrinsic adsorption/desorption step is fast and that adsorption is diffusion-controlled, or closely so.

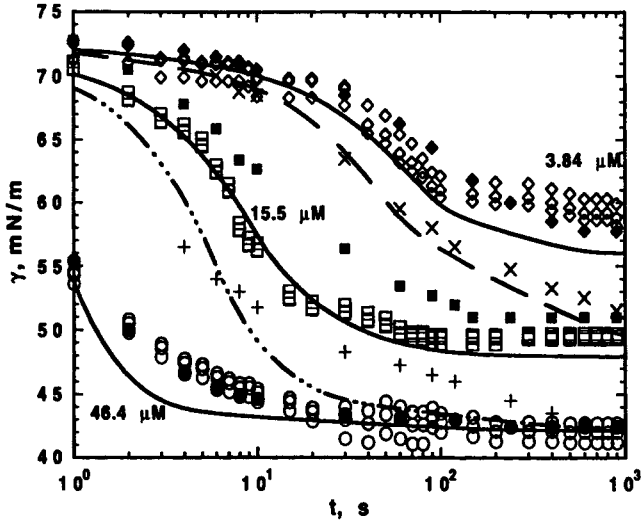

Figure 8. Dynamic surface tensions of aqueous Triton X-100 at 25°C with the PBS method for three independent runs at 3.84 μM (◇), 15.5 μM (□), and 46.4 μM (○).

The estimated error is ±1 mN/m at each run. Data from Chang and Franses (1994a) (3.84 (◆); 15.5 (■); and 46.4 (●) μM), and from Lin et al. (1990) (15.5 (×) and 46.4 (+) μM) are also shown. Solid lines represent data fits to a flat-interface, diffusion-controlled model for $l = 0.02$ cm, for which $N^l = 0.31$ for 3.84 μM, $N^l = 1.5$ for 15.5 μM, and $N^l = 3.35$ for 46.4 μM. Broken lines are calculations for nearly infinite l ($N^l = 100$). $D = 2.6 \times 10^{-10}$ m^2/s.

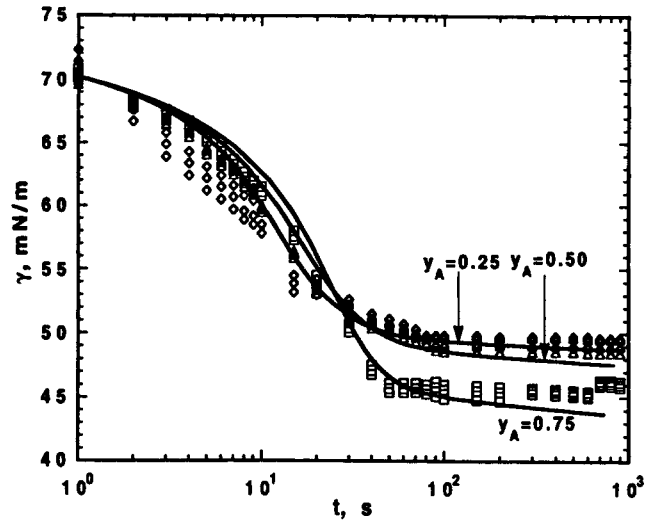

Figure 9. Dynamic surface tensions of aqueous mixtures of $C_{12}E_5$ (*A*) and Triton X-100 (*B*) at $c_T = 15.5$ μM, 25°C, for three independent runs at each y_A ($\equiv c_A/c_T$): 0.25 (◇), 0.50 (△), and 0.75 (□).

The estimated error is ±1 mN/m. The solid lines are calculations for the finite-l model ($l = 0.02$ cm).

The mixture data are compared with the same diffusion-controlled model, with the NAS mixture model for local equilibria and the same D_A, D_B, and l. The equilibrium data for the mixture have been reported earlier (Siddiqui and Franses, 1996a) to yield an interaction parameter, β^σ, of about −0.2, −0.2, and −1.6 for $y_A = 0.25$, 0.50, and 0.75. As discussed by Siddiqui and Franses (1996a), since different values of β^σ were determined at different mole fractions y_A, the regular solution model is not accurate for this mixture, and a more realistic model may be warranted. Nonetheless, to avoid more complexity in the dynamic model, the regular solution equation was used with the β^σ values for each mole fraction given earlier.

Figure 9 shows the data for mixtures of $C_{12}E_5$ (*A*) and Triton X-100 (*B*) at three different mole fractions, for $c_T = 15.5$ μM. The tensions equilibrate within 100 s. For $y_A = 0.75$, the tension is lower at longer times. Tensions calculated with the finite-l diffusion-controlled model agree well with the data, with no additional adjustable parameters. The dynamic surface-tension predictions for the mixtures shown in Figure 9 are shown separately in Figure 10, illustrating more closely the evidence of synergistic dynamic tensions, which are highlighted by thicker lines. Although the mixture with $y_A = 0.75$ is synergistic for $t > 30$ s, the mixtures with $y_A = 0.25$ and 0.50 are synergistic only for short time periods.

The surface-area coverages, fractional-area coverages, concentration profiles, and mole-fraction profiles, for the mixtures in Figure 9 are shown in Figures 11–14. It is possible to obtain predictions at smaller times ($\ll 1$ s) than the data obtainable with the bubble surfactometer (≥ 1 s). The calculated area coverages are larger for Triton X-100 alone than for $C_{12}E_5$ alone. The mixture surface coverages are intermediate between those of the components; no synergism in adsorption is observed at these conditions. The area coverages for the mixtures increase with increasing proportion of Triton X-100. The fractional-area coverages indicate that $\phi_A < y_A$ (Figure 13), that is, an increased coverage of the larger molecules (Triton X-100). However, at longer times (> 100 s) when the monolayer coverage is larger, the smaller molecules ($C_{12}E_5$) are preferentially adsorbed.

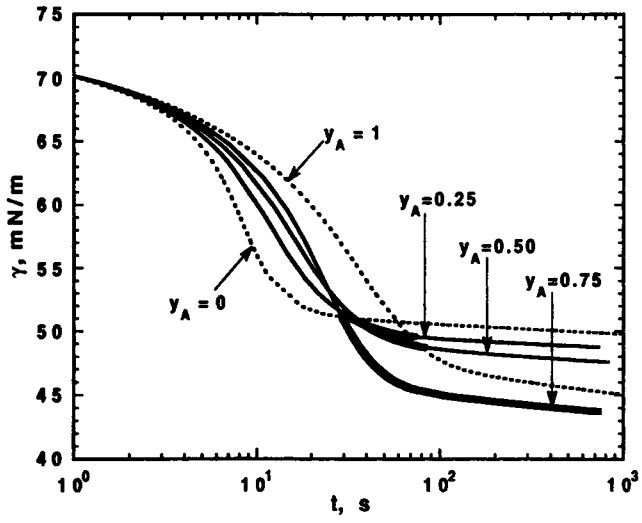

Figure 10. Dynamic surface tension fits for pure components and mixture predictions for aqueous mixtures of $C_{12}E_5$ (*A*) and Triton X-100 (*B*) at $c_T = 15.5$ μM.

For figure clarity, the data from Figure 9 are not shown. The thicker lines indicate the regions of synergism in dynamic or equilibrium tension.

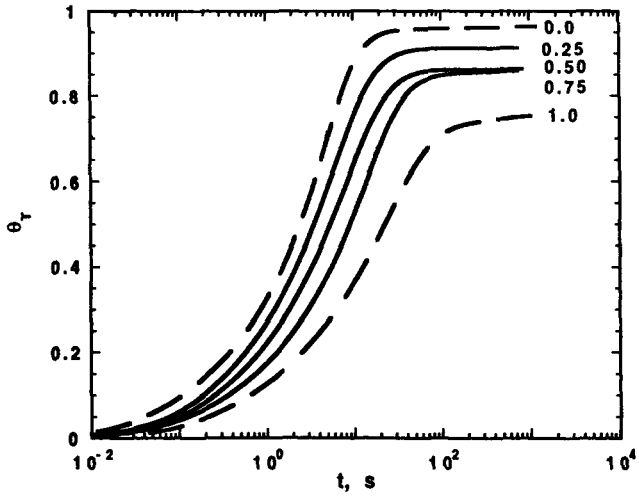

Figure 11. Calculate total area coverages, $\theta_T \equiv \theta_A + \theta_B$, for aqueous mixtures of $C_{12}E_5$ (*A*) and Triton X-100 (*B*) at $c_T = 15.5$ μM.

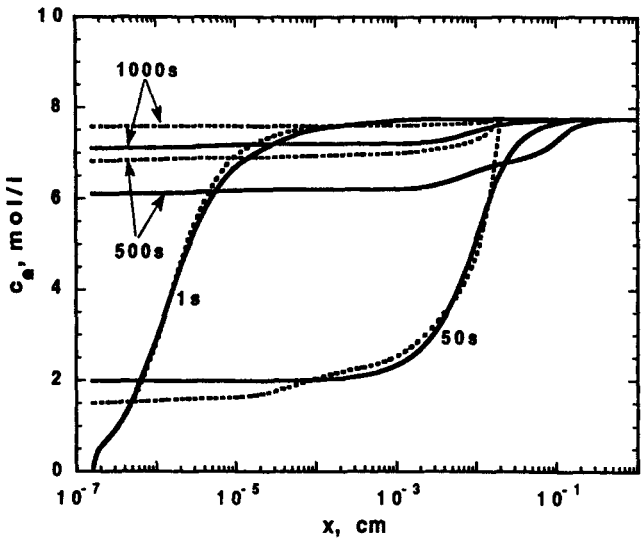

Figure 13. Calculated concentration of $C_{12}E_5$ for the data in Figure 9; *x* is the distance from the interface.

The concentration profiles (Figure 13) show that at 1 s the region immediately below the interface is depleted at the surfactants adsorb to the freshly formed surface. The depleted region grows in thickness (shown by the concentration profile at 50 s) as more surfactant is transported to the interface. At longer times (> 500 s) the bulk phase close to the surface is replenished by transport from regions more distant from the surface. At equilibrium, the subsurface concentration is restored to that of the bulk solution. The predictions for the finite-*l* model (broken line) are similar to those of the infinite-*l* model at small times (< 50 s). At longer times (500 and 1,000 s), the concentration profile changes more rapidly for the finite-length model, since the surfactant needs to diffuse from smaller distances.

The mole fraction y_A^c of $C_{12}E_5$ near the surface depends strongly on time (Figure 14). At 1 s, y_A^c is greater than 0.5, reflecting the preferential adsorption of Triton X-100. At 500 s, this trend is reversed and $C_{12}E_5$ is adsorbed preferentially ($y_A^c < 0.5$), consistently with Figure 12, in which the Triton X-100 concentration at the interface is predicted to have an initial increase followed by a decrease.

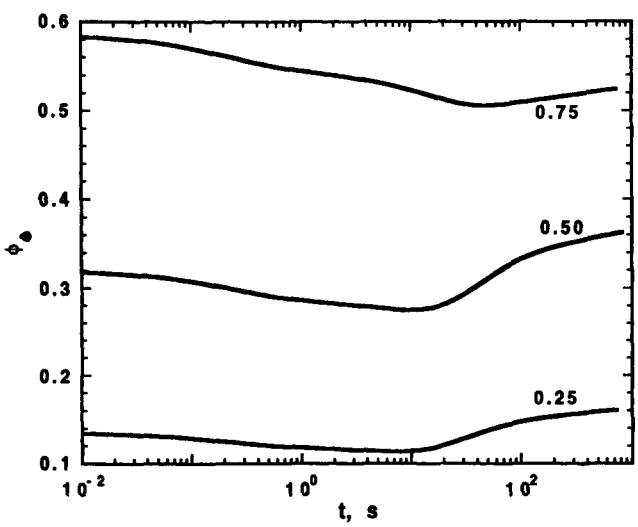

Figure 12. Fractional area coverage, $\phi_A \equiv \theta_A/(\theta_A + \theta_B)$, calculations for aqueous mixtures of $C_{12}E_5$ (*A*) and Triton X-100 (*B*) at $c_T = 15.5$ μM for the data in Figure 9.

Discussion

Most surfactant solutions in practice are formulated as mixtures to achieve various application objectives or to avoid the cost of separating them after synthesis. To optimize surfactant formulations it is important to understand the roles of the various components, and develop and study models for dynamic adsorption and tension.

In this article, a new diffusion-controlled model for dynamic adsorption and tension of nonionic surfactants of different adsorption capacities with nonideal mixing at the

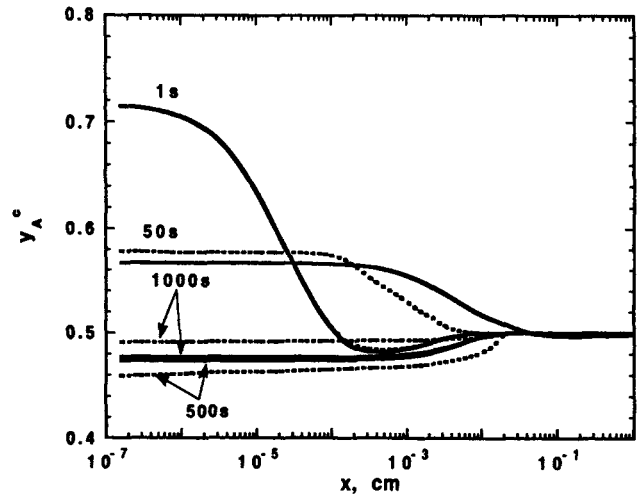

Figure 14. Calculated mole fraction ($x_A \equiv c_A/c_T$) of $C_{12}E_5$ for the data in Figure 9.

interface is presented. For individual surfactants, equilibrium adsorption is adequately characterized by the one-component Langmuir isotherm. For mixtures, the NAS model used considers size differences and nonideal mixing at the interface. This model, original developed by Myers and Prausnitz (1965) for adsorption of gases on solids, has been used to model equilibrium adsorption and tension. One can calculate the adsorbed densities and the relative surface-area coverages at all compositions, if one parameter (β^{σ}) is fitted to some mixture tension data and if the individual component adsorption parameters are used.

Triton X-100 is a nonionic surfactant mixture of different chain lengths, whose tension is well characterized, however, by the one-component Langmuir isotherm. This surfactant is considered as one pseudocomponent. Its dynamic adsorption is diffusion controlled (Hunsel and Joos, 1987; Lin et al., 1990; Fainerman et al., 1994). Equilibrium data for Triton X-100 with the bubble surfactometer agree with previous data (Chang and Franses, 1994a) and with those obtained with the emerging bubble method (Lin et al., 1990). However, dynamic tensions drop faster with the first method, because the effective diffusion-layer thickness is smaller. Detailed models support this argument. New equilibrium and dynamic data for a second nonionic surfactant, $C_{12}E_5$, are also shown to be represented by a finite-thickness diffusion-controlled model and the one-component Langmuir isotherm (Siddiqui and Franses, 1996a; Chang et al., 1992; Carless et al., 1964).

Dynamic tensions for binary mixtures of the preceding components are well represented by the new diffusion-controlled model and the NAS model for local equilibrium at the interface. The parameters used in the model are the adsorption equilibrium parameters, $\Gamma_{m,A}$, $\Gamma_{m,B}$, $K_{L,A}$, $K_{L,B}$; the mixture parameter β^{σ} obtained from equilibrium mixture data; D_A and D_B obtained from the molecular sizes, or from bulk diffusion experiments, and used for the dynamic tensions of the components if adsorption is diffusion-limited (as it is for the example used here); and the diffusion length l, which stems from the bubble surfactometer geometry and fits well the dynamic data of the components.

The new model indicates preferential adsorption of the larger molecules at short times and of the smaller molecules at longer times, if K_L and D are equal. The dynamic adsorption selectivity is reduced when there are negative deviations from ideal mixing (net attractive interactions). In fact, when $\beta^{\sigma} < 0$ synergism in tension equilibrium is possible (Siddiqui and Franses, 1996b). Moreover, synergism in dynamic tension is modeled and observed here for the first time.

Conclusions

A new diffusion-controlled model for dynamic adsorption and tension of binary soluble surfactants at the air/water interface has been developed. The model accounts for differences in adsorption capacities and nonideal mixing in the monolayer. If K_L and D are equal, then at short times the larger molecules tend to be preferentially adsorbed at the interface, while at long times the smaller molecules tend to be preferred. This "desorption" of the larger molecules is attributed to the primarily entropic effect of adsorption capacity and surface pressure. A finite-thickness model was used to successfully explain the faster decrease in tension data obtained with a bubble surfactometer. A new phenomenon, called dynamic surface-tension synergism, defined as having lower tension than the individual components at the same total concentration and at the same time, is observed. It is mostly due to mixing in the monolayer with negative deviations from ideality and to differences in adsorption capacities. The results can be used for formulating more effective surfactant mixtures with a better understanding of the surface coverages of the components.

Acknowledgments

This research was supported in part by National Science Foundation Grants BCS 91-12154 and CTS 93-04328, and by the Purdue Research Foundation.

Notation

l = thickness of the diffusion layer, m
$\mathcal{R}$ = universal gas constant, 8.314 J/K
R = radius of the bubble, m
R_{Γ} = ratio of adsorption capacities ($\Gamma_{m,1}/\Gamma_{m,2}$)
T = temperature, K
t = time, s
x = distance from the surface into the bulk, m
γ_0 = surface tension of the pure solvent, mN/m
$\bar{\Gamma}_i$ = dimensionless surface density (Γ_i/Γ_i^e)

Literature Cited

Baret, J. F., "Kinetics of Adsorption from a Solution. Role of the Diffusion and of the Adsorption-Desorption Antagonism," *J. Phys. Chem.*, **72**, 2755 (1968).

Bikerman, J. J., *Foams*, Springer-Verlag, New York (1973).

Bird, R. B., W. E. Stewart, and E. N. Lightfoot, *Transport Phenomena*, Wiley, New York, p. 514 (1960).

Borwankar, R. P., and D. T. Wasan, "The Kinetics of Adsorption of Surface Active Agents at Gas-Liquid Surfaces," *Chem. Eng. Sci.*, **38**, 1637 (1983).

Broughton, D. R., "Adsorption Isotherms for Binary Gas Mixtures," *Ind. Eng. Chem.*, **40**, 1506 (1948).

Carless, J. E., R. A. Challis, and B. A. Mulley, "Nonionic Surface-Active Agents. Part V. The Effect of the Alkyl and the Polyglycol Chain Length on the Critical Micelle Concentration of Some Monoalkyl Polyethers," *J. Colloid Sci.*, **19**, 201 (1964).

Chang, C. H., and E. I. Franses, "Modified Langmuir-Hinshelwood Kinetics for Dynamic Adsorption of Surfactants at the Air/Water Interface," *Colloids Surfaces*, **69**, 189 (1992).

Chang, C. H., and E. I. Franses, "An Analysis of the Factors Affecting Dynamic Tension Measurements with the Pulsating Bubble Surfactometer," *J. Colloid Interf. Sci.*, **164**, 107 (1994a).

Chang, C. H., and E. I. Franses, "Dynamic Tension Behavior of Aqueous Octanol Solutions under Constant-Area and the Pulsating-Area Conditions," *Chem. Eng. Sci.*, **49**, 313 (1994b).

Chang, C. H., and E. I. Franses, "Adsorption Dynamics of Surfactants at the Air/Water Interface: A Critical Review of Mathematical Models, Data and Mechanisms," *Colloids Surfaces A*, **100**, 1 (1995).

Chang, C. H., N.-H. L. Wang, and E. I. Franses, "Adsorption Dynamics of Single and Binary Surfactants at the Air/Water Interface," *Colloids Surfaces*, **62**, 321 (1992).

Defay, R., and G. Petré, "Dynamic Surface Tension," *Surface and Colloid Science*, Vol. 3, E. Matijevic, ed., Wiley, New York (1971).

Dukhin, S. S., G. Kretzschmar, and R. Miller, *Dynamics of Adsorption at Liquid Interfaces*, Elsevier, New York (1995).

Enhorning, G., "Pulsating Bubble Techniques for Evaluating Pulmonary Surfactant," *J. Appl. Physiol.: Respirat. Environ. Exercise Physiol.*, **43**, 198 (1977).

Fainerman, V. B., "Kinetics of Adsorption of Ionic Surfactants at the Solution-Air Interface and the Nature of the Adsorption Barrier," *Colloids Surfaces*, **57**, 249 (1991).

Fainerman, V. B., A. V. Makievski, and P. Joos, "Adsorption Kinetics of Octylphenyl Ethers of Poly(ethylene glycol)s on the Solution-Air Interface," *Colloids Surfaces A*, **90**, 213 (1994).
Fainerman, V. B., and R. Miller, "Dynamic Surface Tensions of Surfactant Mixtures at Water-Air Interface," *Colloids Surfaces A*, **97**, 65 (1995).
Franses, E. I., F. A. Siddiqui, D. J. Ahn, C. H. Chang, and N.-H. L. Wang, "Thermodynamically Consistent Equilibrium Adsorption Isotherms for Mixtures of Different-Size Molecules," *Langmuir*, **90**, 1236 (1995).
Frisch, H. L., and K. J. Mysels, "Diffusion-Controlled Adsorption. Concentration Kinetics, Ideal Isotherms, and Some Applications," *J. Phys. Chem.*, **87**, 3988 (1983).
Garrett, P. R., and P. L. Gratton, "Dynamic Surface Tensions, Foam and the Transition from Micellar Solution to Lamellar Phase Dispersion," *Colloids Surfaces A*, **103**, 127 (1995).
Hua, X. Y., and M. J. Rosen, "Dynamic Surface Tension of Aqueous Surfactant Solutions. I. Basic Parameters," *J. Colloid Interf. Sci.*, **124**, 652 (1988).
Hunsel, J. V., and P. Joos, "Adsorption Kinetics at the Oil/Water Interface," *Colloids Surfaces*, **24**, 139 (1987).
Kretzschmar, G., and R. Miller, "Dynamic Properties of Adsorption Layers of Amphiphilic Substances at Fluid Interfaces," *Adv. Colloid Interf. Sci.*, **36**, 65 (1991).
LeVan, M. D., and T. Vermeulen, "Binary Langmuir and Freundlich Isotherms for Ideal Adsorbed Solutions," *J. Phys. Chem.*, **85**, 3247 (1981).
Lin, S. Y., K. McKeigue, and C. Maldarelli, "Diffusion-Controlled Surfactant Adsorption Studied by Pendant Drop Digitization," *AIChE J.*, **36**, 1785 (1990).
Miller, R., P. Joos, and V. B. Fainerman, "Dynamic Surface and Interfacial Tensions of Surfactant and Polymer Solutions," *Adv. Colloid Interf. Sci.*, **49**, 249 (1994).
Miller, R., and G. Kretzschmar, "Numerical Solution for a Mixed Model of Diffusion Kinetics-Controlled Adsorption," *Colloid Poly. Sci.*, **258**, 85 (1980).
Myers, A. L., and J. M. Prausnitz, "Thermodynamics of Mixed-Gas Adsorption," *AIChE J.*, **11**, 121 (1965).
Notter, R. H., and J. N. Finkelstein, "Pulmonary Surfactant: An Interdisciplinary Approach," *J. Appl. Physiol., Respir. Environ. Exercise Physiol.*, **57**, 1613 (1984).
Prausnitz, J. M., R. N. Lichtenthaler, and E. G. de Azevedo, *Molecular Thermodynamics of Fluid-Phase Equilibria*, 2nd ed., Prentice Hall, Englewood Cliffs, NJ (1986).
Scheindorf, C., M. Rebhum, and M. Sheintuch, "A Freundlich-type Multicomponent Isotherm," *J. Colloid Interf. Sci.*, **79**, 136 (1981).
Schwuger, M. J., "Effects of Adsorption on Detergency Phenomena: I," *J. Amer. Oil Chem. Soc.*, **59**, 258 (1982).
Siddiqui, F. A., "Dynamic Adsorption and Tension of Mixed Nonionic Surfactants at the Air/Water Interface," PhD Thesis, Purdue Univ., West Lafayette, IN (1996).
Siddiqui, F. A., and E. I. Franses, "Equilibrium Adsorption and Tension of Binary Surfactant Mixtures at the Air/Water Interface," *Langmuir*, **12**, 354 (1996a).
Siddiqui, F. A., and E. I. Franses, "Surface Tension and Adsorption Synergism for Solutions of Binary Surfactants," *Ind. Eng. Chem. Res.*, **35**, 3223 (1996b).
Sutherland, K. L., "The Kinetics of Adsorption at Liquid Surfaces," *Aust. J. Sci. Res. Ser. A*, **5**, 683 (1952).
Thomas, L. H., "Elliptic Problems in Linear Difference Equations over a Network," Tech. Rep., Watson Scientific Computing Laboratory Report, New York (1949).
Tsonopoulos, C., J. Newman, and J. M. Prausnitz, "Rapid Aging and Dynamic Surface Tension of Dilute Aqueous Solutions," *Chem. Eng. Sci.*, **26**, 817 (1971).
Valentini, J. E., W. R. Thomas, P. Sevenhuysen, T. S. Jiang, H. O. Lee, L. Yi, and S. C. Yen, "Role of Dynamic Surface Tension in Slide Coating," *Ind. Eng. Chem. Res.*, **30**, 453 (1991).
Van den Bogaert, R., and P. Joos, "Diffusion-Controlled Adsorption Kinetics for a Mixture of Surface Active Agents at the Solution-Air Interface," *J. Phys. Chem.*, **80**, 190 (1980).
Ward, A. F. H., and L. Tordai, "Time-Dependence of Boundary Tensions of Solutions. I. The Role of Diffusion in Time-Effects," *J. Chem. Phys.*, **14**, 453 (1946).
Ziller, M., and R. Miller, "On the Solution of Diffusion Controlled Adsorption Kinetics by Means of Orthogonal Collocation," *Colloid Poly. Sci.*, **264**, 611 (1986).

Manuscript received Oct. 24, 1996, and revision received Jan. 21, 1997.